

# Vibrations in jammed solids: Beyond linear response

Thibault Bertrand<sup>1</sup>, Carl F. Schreck<sup>1,2</sup>, Corey S. O’Hern<sup>1,2,3</sup>, and Mark D. Shattuck<sup>4,1</sup>

<sup>1</sup>*Department of Mechanical Engineering & Materials Science,  
Yale University, New Haven, Connecticut 06520-8260, USA*

<sup>2</sup>*Department of Physics, Yale University, New Haven, Connecticut 06520-8120, USA*

<sup>3</sup>*Department of Applied Physics, Yale University, New Haven, Connecticut 06520-8120, USA and*

<sup>4</sup>*Benjamin Levich Institute and Physics Department,*

*The City College of the City University of New York, New York, New York 10031, USA*

We propose a ‘phase diagram’ for particulate systems that interact via purely repulsive contact forces, such as granular media and colloidal suspensions. We identify and characterize two distinct classes of behavior as a function of the input kinetic energy per degree of freedom  $T_0$  and packing fraction deviation above and below jamming onset  $\Delta\phi = \phi - \phi_J$  using numerical simulations of purely repulsive frictionless disks. Iso-coordinated solids (ICS) only occur above jamming for  $\Delta\phi > \Delta\phi_c(T_0)$ ; they possess average coordination number equal to the isostatic value ( $\langle z \rangle = z_{\text{iso}}$ ) required for mechanically stable packings. ICS display harmonic vibrational response, where the density of vibrational modes from the Fourier transform of the velocity autocorrelation function is a set of sharp peaks at eigenfrequencies  $\omega_k^d$  of the dynamical matrix evaluated at  $T_0 = 0$ . Hypo-coordinated solids (HCS) occur both above and below jamming onset within the region defined by  $\Delta\phi > \Delta\phi_-^*(T_0)$ ,  $\Delta\phi < \Delta\phi_+^*(T_0)$ , and  $\Delta\phi > \Delta\phi_{cb}(T_0)$ . In this region, the network of interparticle contacts fluctuates with  $\langle z \rangle \approx z_{\text{iso}}/2$ , but cage-breaking particle rearrangements do not occur. The HCS vibrational response is nonharmonic, *i.e.* the density of vibrational modes  $D(\omega)$  is not a collection of sharp peaks at  $\omega_k^d$ , and its precise form depends on the measurement method. For  $\Delta\phi > \Delta\phi_{cb}(T_0)$  and  $\Delta\phi < \Delta\phi_-^*(T_0)$ , the system behaves as a hard-particle liquid.

PACS numbers: 63.50.Lm, 63.50.-x, 64.70.pv, 83.80.Fg

The vibrational response of conventional solids, such as metals, ceramics, and minerals, can be described by linear response at sufficiently low temperatures compared to the melting points [1]. Nonlinearities stemming from weak structural disorder and the shape of the interaction potential explored at low temperatures can be treated as small perturbations to the description of the harmonic solid [2]. Particulate systems, such as granular media [3] and colloids [4], can also exist in solid-like states in the limit of weak driving or thermal fluctuations. However, in contrast to molecular-scale solids, the interactions in many particulate solids are purely repulsive and vanish when particles come out of contact. We have shown previously [5] that even small changes in the contact network in purely repulsive particle-based solids give rise to strong nonlinearities in the measured vibrational response that are not found in conventional solids.

In spite of these nonlinearities, a major emphasis of the jamming literature in the past decade has been to invoke linear response of static packings to provide insight into the structural relaxation of dense liquids near the glass transition [6, 7]. However, one of the most obvious and important questions has been left unanswered: what is the measured response of static packings near jamming onset when they are subjected to vibrations? In this Letter, we do not rely on linear response to infer vibrational behavior. Instead, we measure directly the vibrations of model particulate systems as a function of  $\Delta\phi = \phi - \phi_J$  above and below jamming and input kinetic energy  $T_0$ .

We identify two distinct classes of behavior in the  $\Delta\phi$  and  $T_0$  plane near jamming as shown in Fig. 1: iso- and hypo-coordinated solids (ICS and HCS), which are dis-

tinguished by the time-averaged contact number  $\langle z \rangle$  and density of vibrational modes  $D(\omega)$ . We focus on the regime where there are no cage-breaking particle rearrangements. For the ICS, with  $\Delta\phi > \Delta\phi_c(T_0) > 0$ , the contact network does not change from that at  $T_0 = 0$ , and the vibrational response is harmonic with strong peaks in the Fourier transform of the velocity autocorrelation function at the dynamical matrix eigenfrequencies. HCS occur both above and below  $\phi_J$  [8] in the region defined by  $\Delta\phi > \Delta\phi_-^*(T_0)$ ,  $\Delta\phi < \Delta\phi_+^*(T_0)$ , and  $\Delta\phi > \Delta\phi_{cb}(T_0)$ . In the HCS, the network of interparticle contacts fluctuates with an average contact number at approximately half of the isostatic value ( $\langle z \rangle / z_{\text{iso}} \approx 0.5$ ), the vibrational response is strongly nonharmonic, and the form of  $D(\omega)$  depends on the measurement method. In the regime  $\Delta\phi > \Delta\phi_{cb}(T_0)$  and  $\Delta\phi < \Delta\phi_-^*(T_0)$ ,  $\langle z \rangle / z_{\text{iso}} \sim 0$ , and  $D(\omega)$  resembles that for hard-particle liquids (HPL).

*Model and Simulations* We measure the vibrational response of mechanically stable (MS) packings of  $N$  bidisperse frictionless disks with mass  $m$  that interact via the pairwise purely repulsive potential

$$V(r_{ij}) = \frac{\epsilon}{2} \left( 1 - \frac{r_{ij}}{\sigma_{ij}} \right)^2 \Theta \left( 1 - \frac{r_{ij}}{\sigma_{ij}} \right), \quad (1)$$

where  $r_{ij}$  is the separation between disk centers,  $\sigma_{ij} = (\sigma_i + \sigma_j)/2$  is the average disk diameter,  $\epsilon$  is the energy scale of the repulsive interaction, and  $\Theta(x)$  is the Heaviside step function. The bidisperse mixtures contained half large and half small disks by number with diameter ratio  $r = \sigma_2/\sigma_1 = 1.4$ . We focus on the  $\Delta\phi \rightarrow 0$  limit for which the MS packings possess the isostatic number of

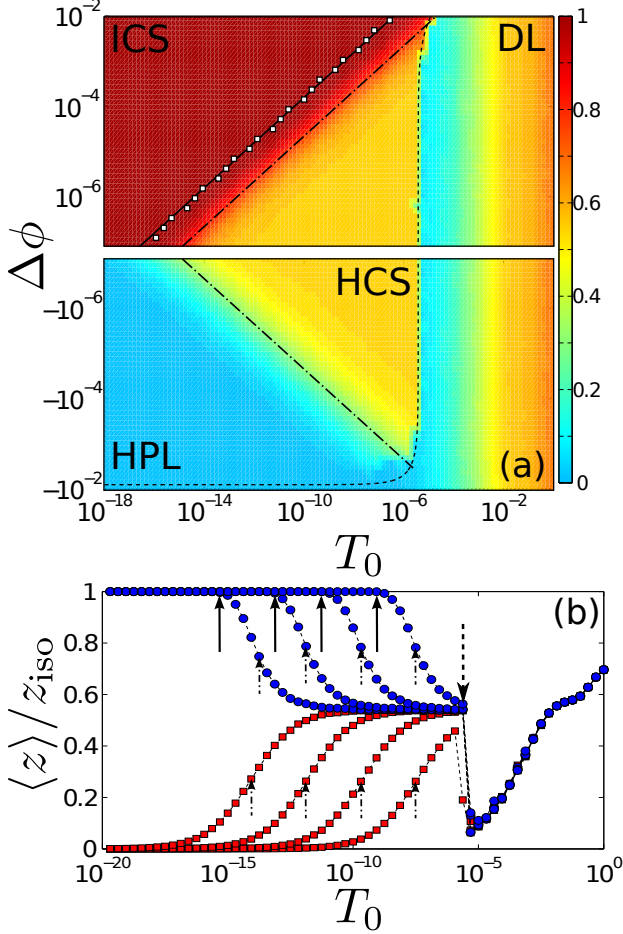


FIG. 1: (Color online) (a) ‘Phase diagram’ for the vibrational response of MS packings versus  $\Delta\phi$  and  $T_0$  illustrated for  $N = 10$ . The shading gives the time-averaged contact number  $\langle z \rangle / z_{\text{iso}}$ . For  $0 < \Delta\phi(T_0) < \Delta\phi_c(T_0)$  (data and scaling curve given by open squares and solid line, respectively), the contact network for the ‘ICS’ does not change from that at  $T_0 = 0$  and the vibrational response is harmonic. The mid-points  $T_0$  at which  $\langle z \rangle / z_{\text{iso}}$  crosses over from 1 to 0.5 and from 0 to  $\approx 0.5$ , which define  $\Delta\phi_{\pm}^*(T_0)$ , are indicated by dot-dashed lines (with slope  $\pm 0.5$ ). In the ‘HCS’ and ‘HPL’ regions, the contact network fluctuates with  $\langle z \rangle / z_{\text{iso}} \approx 0.5$  and 0, respectively, but there are no particle rearrangements as in the ‘DL’ regime with  $\Delta\phi < \Delta\phi_{cb}(T_0)$  (dashed line). (b)  $\langle z \rangle / z_{\text{iso}}$  versus  $T_0$  for  $\Delta\phi = \pm 10^{-7}$ ,  $\pm 10^{-6}$ ,  $\pm 2 \times 10^{-5}$ , and  $\pm 2 \times 10^{-4}$  (circles and squares) from left to right. The solid, dot-dashed, and dashed arrows indicate  $\Delta\phi_c(T_0)$ ,  $\Delta\phi_{\pm}^*(T_0)$ , and  $\Delta\phi_{cb}(T_0)$ , respectively, in (a).

interparticle contacts  $N_c^{\text{iso}} = 2N - 1$ , where  $N = N' - N_r$ , and  $N$  is the number of particles after  $N_r$  rattler particles with fewer than 3 contacts have been removed.

We generate MS packings at  $\Delta\phi_0 = 10^{-8}$  using the successive compression and decompression protocol described previously [9] for system sizes in the range  $N = 10$  to 512. Each of these packings were then decompressed or overcompressed in a single step to a given  $\Delta\phi$  in

the range  $-10^{-2} \leq \Delta\phi \leq 10^{-2}$  followed by conjugate gradient energy minimization to the configuration  $\vec{R}^0 = \{x_1^0, y_1^0, \dots, x_N^0, y_N^0\}$ .

We perturbed each system at  $\vec{R}^0$  by exciting equal kinetic energy in each mode. We selected the initial particle velocities  $\vec{v} = \{v_{xi}, v_{yi}, \dots, v_{xN}, v_{yN}\}$  according to

$$v_n = \delta \sum_{k=1}^{2N-2} e_n^k, \quad (2)$$

where  $\hat{e}^k$  are the  $2N - 2$  eigenvectors (corresponding to the nonzero eigenvalues) of the dynamical matrix [10] evaluated at  $\vec{R}^0$ ,  $(\hat{e}^k)^2 = 1$ , and  $\delta$  is chosen so that the normalized kinetic energy  $T_0 = \epsilon^{-1} \sum_i \frac{1}{2} m v_i^2 / (2N - 2)$  is in the range  $10^{-20} \leq T_0 \leq 10^{-1}$ . We then integrated Newton’s equations of motion at constant total energy and area in a square box with side length  $L = 1$  using the velocity Verlet algorithm with time step  $\Delta t = 1 / (400\pi) \sigma_1 \sqrt{m / \epsilon}$ . We first ran the constant energy simulations for  $10^3$  oscillations of the lowest dynamical matrix eigenfrequency  $\omega_1^d$  and then quantified fluctuations in the particle positions over the next  $10^3$  periods.

In the harmonic regime, the time-dependent particle positions are described by

$$R_n(t) = R_n^0 + \sum_{k=1}^{2N-2} \tilde{R}_k e_n^k \cos(\omega_k t + \psi_k), \quad (3)$$

where  $\tilde{R}_k$  are the time-independent amplitudes of the normal modes  $\hat{e}_k$  with eigenfrequency  $\omega_k^d$  from the dynamical matrix. We employed two additional methods to measure the vibrational response as a function of  $\Delta\phi$  and  $T_0$ . We calculated the Fourier transform of the normalized velocity autocorrelation function to quantify the density of vibrational modes [12]

$$D(\omega^v) = \int_0^\infty dt \frac{\langle \vec{v}(t_0 + t) \cdot \vec{v}(t_0) \rangle}{\langle \vec{v}(t_0) \cdot \vec{v}(t_0) \rangle} e^{i\omega t}, \quad (4)$$

where  $\langle \cdot \rangle$  indicate averages over all particles and time origins  $t_0$ . We also measured the eigenvalue spectrum of  $S = VC^{-1}$  (which equals the dynamical matrix  $M$  provided Eq. 3 holds), where  $V_{ij} = \langle v_i v_j \rangle$  are the elements of the velocity matrix,

$$C_{ij} = \langle (R_i - R_i^0)(R_j - R_j^0) \rangle \quad (5)$$

are the elements of the displacement correlation matrix [13], and angle brackets indicate averages over time. Vibrational frequencies  $\omega_k^s = \sqrt{s_k}$  can be obtained from the eigenvalues of  $S$ . The binned versions of the density of vibrational frequencies are given by  $D(\omega^{s,d}) = [\mathcal{N}(\omega^{s,d} + \Delta\omega^{s,d}) - \mathcal{N}(\omega^{s,d})] / (\mathcal{N}(\infty) \Delta\omega^{s,d})$ , where  $\mathcal{N}(\omega)$  is the number of frequencies less than  $\omega$ .  $D(\omega^d)$ ,  $D(\omega^v)$ , and  $D(\omega^s)$  are normalized so that  $\int_0^\infty d\omega D(\omega) = 1$ .

*Results* In the harmonic vibrational response regime for MS packings, the fluctuating particle positions are given

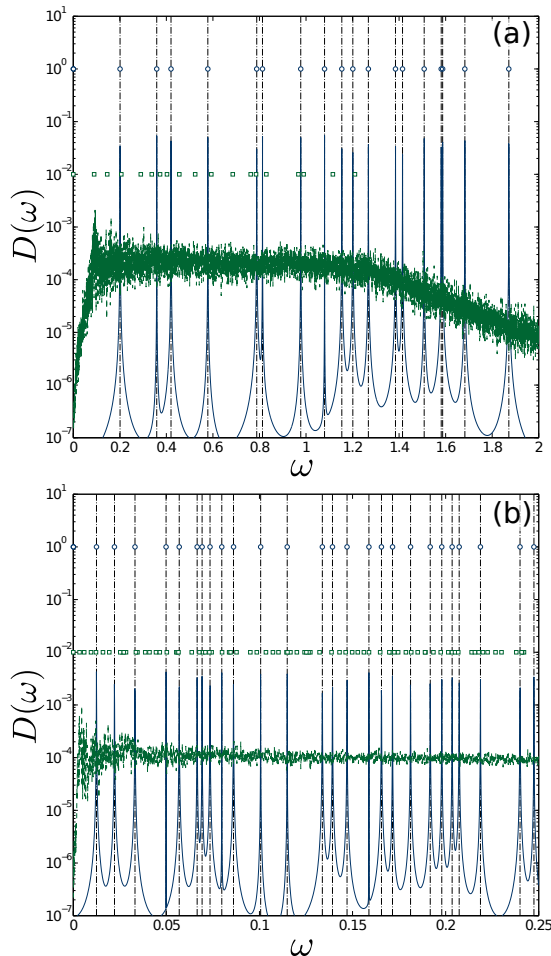


FIG. 2: (Color online) Comparison of portions of the density of vibrational frequencies  $D(\omega)$  from the Fourier transform of the velocity autocorrelation function (lines) and associated with the dynamical (vertical dot-dashed lines) and displacement correlation matrices (symbols) for the ICS at  $\Delta\phi = 2 \times 10^{-7}$  and  $T_0 = 4 \times 10^{-19}$  (blue solid lines and circles) and HCS at  $\Delta\phi = 2 \times 10^{-7}$  and  $T_0 = 2 \times 10^{-11}$  (green dashed lines and squares) for (a)  $N = 10$  and (b) 128.

by Eq. 3, and  $D(\omega^v)$  from the Fourier transform of the velocity autocorrelation function is a set of  $2N - 2$  spikes at frequencies  $\omega_k^v$ , which correspond to the eigenfrequencies associated with the dynamical and displacement correlation matrices, and become  $\delta$ -functions in the  $T_0 = 0$  limit,  $D(\omega^v) = \sum_{k=1,2N-2} \delta(\omega^v - \omega_k^{d,s})$ . In Fig. 2, we show  $D(\omega^v)$  for MS packings at  $\Delta\phi > 0$ , two  $T_0$ , and two system sizes. For sufficiently low  $T_0$  in the ICS, the system displays harmonic response with  $\omega_k^v = \omega_k^{d,s}$ . For larger  $T_0$ , the instantaneous contact network deviates from that at  $T_0 = 0$ , and the vibrational response becomes nonharmonic. We find that  $\omega_k^s < \omega_k^d$  (assuming the eigenvalues are sorted from smallest to largest),  $D(\omega^v)$  becomes a *continuous* spectrum, and none of the densities of vibrational frequencies ( $D(\omega^v)$ ,  $D(\omega^s)$ , and  $D(\omega^d)$ ) match. The same behavior is found for both  $N = 10$  and 128.

In Fig. 3 (a) we show the dependence of the frequencies  $\omega_k^s$  associated with the displacement correlation matrix versus  $T_0$  and  $\Delta\phi$  for a  $N = 10$  MS packing above and below jamming onset. As shown in panel (a) for  $\Delta\phi > 0$ ,  $\omega_k^s = \omega_k^d$  for all  $k$  in the ICS when  $T_0 < T_c(\Delta\phi)$ . For  $T_0 > T_c(\Delta\phi)$  and  $\Delta\phi > 0$ , the frequencies  $\omega_k^s$  first decrease with  $T_0$  and then each reaches a  $k$ -dependent plateau value  $\omega_k^* < \omega_k^d$  that persists for more than six orders of magnitude (at  $\Delta\phi = 10^{-6}$ ). The plateau ends abruptly after a particle rearrangement occurs at  $T_{cb}(\Delta\phi)$ . Cage-breaking rearrangements were identified by comparing the particle positions for energy minimized configurations  $\vec{R}^{\min}$  originally at  $T_0 > 0$  to those for the MS packing  $\vec{R}^0$  at  $T_0 = 0$ . For  $T_0 < T_{cb}(\Delta\phi)$ , the distribution  $P(\Delta R)$  of configurational distances  $\Delta R = \sqrt{(2N)^{-1} \sum_{i=1}^N [(x_i^{\min} - x_i^0)^2 + (y_i^{\min} - y_i^0)^2]}$  [11] has a strong peak at small  $\Delta R/\sigma_1 \sim 10^{-7}$  that corresponds to the precision of the particle positions after energy minimization. For both  $\Delta\phi > 0$  and  $\Delta\phi < 0$ ,  $P(\Delta R)$  is bimodal for  $T \gtrsim T_{cb}(\Delta\phi)$  with an additional well-separated peak at larger  $\Delta R$  from cage-breaking particle rearrangements. (See supplementary material.)

In contrast, for  $\Delta\phi \leq 0$ , there is no harmonic vibrational response regime. We find that the frequencies  $\omega_k^s$  increase from zero at  $T_0 = 0$  and reach the same  $k$ -dependent plateau values  $\omega_k^*$  as those for  $\Delta\phi > 0$ . These results point to a robust set of frequencies (distinct from  $\omega_k^d$ ) in the HCS regime, where the contact network fluctuates, but the average contact number remains constant near  $\langle z \rangle / z_{\text{iso}} \approx 0.5$ .

Motivated by the behavior in the regime  $\Delta\phi < 0$ , for which the frequencies  $\omega_k^s \sim \sqrt{T_0}/l_c(\Delta\phi)$  scale as the ratio of the velocity between interparticle collisions and typical cage size and then reach a plateau  $\omega_k^*$  at large  $T_0$ , we propose the following scaling function:

$$\omega_k^s = \omega_k^* \left( 1 + \frac{l_c(\Delta\phi)}{\sqrt{T_0}} \right)^{-1}, \quad (6)$$

where  $l_c$  is measured in units of  $\sigma_1$ . In Fig. 3 (b), we show least-squares fits of the maximum frequency associated with the displacement correlation matrix  $\omega_m^s$  versus  $T_0$  to Eq. 6 for 28 logarithmically-spaced packing fraction deviations below jamming in the range  $10^{-7} \leq |\Delta\phi| \leq 10^{-2}$ . (Similar quality fits are found for all lower frequencies.) Above jamming,  $\omega_k^s$  interpolates between  $\omega_k^d$  at  $T_0 = 0$  and  $\omega_k^*$  at large  $T_0$ . The generalized logistic function,

$$\omega_k^s(T_0) = \omega_k^d + \frac{\omega_k^* - \omega_k^d}{(1 + l_c(\Delta\phi)/T_0^\alpha)^\nu}, \quad (7)$$

which allows variations of the slope of  $\omega_k^s(T_0)$  in the crossover region, is able to recapitulate  $\omega_m^s$  both below and above jamming (Fig. 3 (b)). Below jamming, the best fits give  $\alpha = 0.5$  and  $\nu = 1$  (*i.e.* Eq. 6). Above jamming, we find  $\alpha \sim 0.6$  and  $\nu \approx 0.25l_c^{-1/2}$  over a wide range of  $\Delta\phi$ . In Fig. 3 (c), we show that Eq. 7 collapses  $\omega_m^s$  from panel (b) with some deviation at small  $T_0$  for

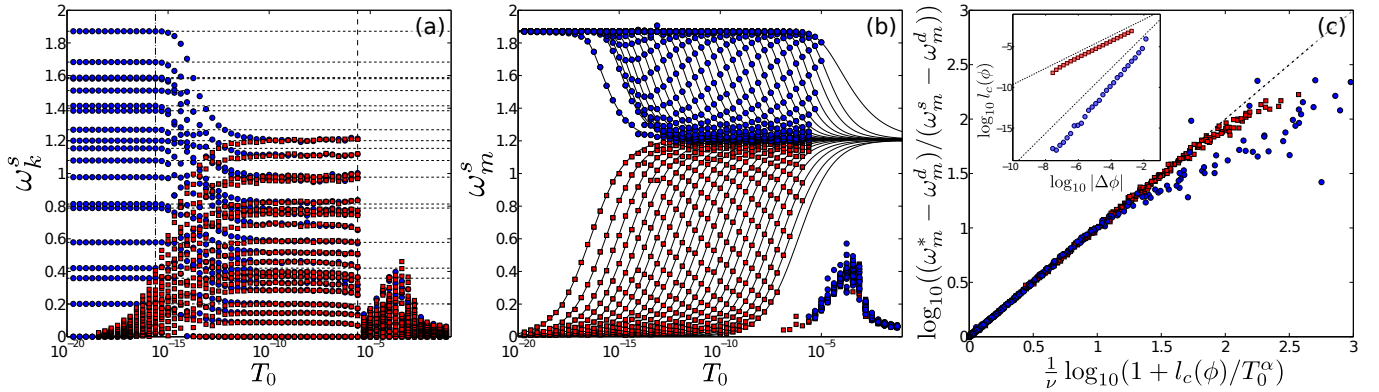


FIG. 3: (Color online) (a) The  $2N - 2$  nontrivial frequencies  $\omega_k^s$  associated with the displacement correlation matrix versus  $T_0$  for  $\Delta\phi = 10^{-6}$  (blue circles) and  $-10^{-6}$  (red squares) for  $N = 10$ . The vertical dot-dashed and dashed lines indicate for  $\Delta\phi = 10^{-6}$  the  $T_c$  where the contact network first differs from that at  $T_0 = 0$  and  $T_{cb}$  where the energy-minimized configurations differ from that at  $T_0 = 0$ , respectively. The horizontal dashed lines show the dynamical matrix eigenfrequencies. (b) The maximum frequency  $\omega_m^s = \max_k \omega_k^s$  versus  $T_0$  for 28 packing fraction deviations logarithmically spaced in the range  $10^{-7} \leq |\Delta\phi| \leq 10^{-2}$  above and below jamming. The solid lines are fits of  $\omega_m^s(T_0)$  to Eq. 7. (c) Scaled  $\omega_m^s$  versus  $T_0$ . The inset shows  $l_c$  versus  $|\Delta\phi|$  above and below jamming. The dashed and dotted lines have slope 1 and 2, respectively.

systems above jamming (caused by numerical accuracy when  $\omega_m^s \approx \omega_m^d$ ). In the inset to panel (c), we show that the generalized cage size scales as  $l_c \sim \Delta\phi$  below and  $\sim (\Delta\phi)^\lambda$  with  $\lambda \gtrsim 2$  above jamming.

We summarize our results for the measured vibrational response of MS packings in the ‘phase diagram’ in Fig. 1. For  $\Delta\phi > \Delta\phi_c(T_0) \sim N^\beta \sqrt{T_0}/A$  (see Ref. [5]), where  $A \approx 0.5$  and  $\beta \approx 0.85$ , the contact network does not change from that at  $T_0 = 0$ . In the ICS,  $\langle z \rangle = z_{\text{iso}}$ , the vibrational response is harmonic, and the density of vibrational modes  $D(\omega^v) = D(\omega^s) = D(\omega^d)$  (Fig. 4 (a)). Note that the size of the ICS region decreases with increasing  $N$ . In Fig. 1, we show that the midpoints of the crossovers in  $\langle z \rangle/z_{\text{iso}}$  from 1 to 0.5, which define  $\Delta\phi_+^*(T_0)$ , scale as  $\sqrt{T_0}$ . Assuming that the effective particle diameter shrinks with  $\sqrt{T_0}$  [14], we obtain an estimate for the shift in  $\phi_J$  induced by thermal fluctuations:

$$\Delta\phi_s(T_0) = \phi_J \left( \frac{1}{(1 - \sqrt{2T_0})^2} - 1 \right). \quad (8)$$

We find that near this boundary  $\Delta\phi_s \sim \Delta\phi_+^*$  an extensive number of changes in the contact network from that at  $T_0 = 0$  has occurred. Similarly, for  $\Delta\phi < 0$ , an extensive number of ‘time-averaged’ contacts has formed when  $\Delta\phi > \Delta\phi_-^*(T_0)$ , which also scales as  $\sqrt{T_0}$ . In Fig. 4 (b), we show the density of vibrational frequencies for 75 sets of parameters in the HCS region  $\Delta\phi > \Delta\phi_-^*(T_0)$ ,  $\Delta\phi < \Delta\phi_+^*(T_0)$ , and  $\Delta\phi > \Delta\phi_{cb}(T_0)$ . We find that  $D(\omega^s) \neq D(\omega^v)$ , *e.g.*  $D(\omega^s)$  possesses a stronger peak at low frequencies and opposite curvature at high frequencies. In contrast,  $D(\omega^s)$  and  $D(\omega^v)$  each separately can be collapsed for HPL by scaling by the average frequency,

but this does not mean that the system is harmonic [12]. In the transition regime,  $\Delta\phi_c(T_0) < \Delta\phi < \Delta\phi_+^*(T_0)$ ,  $D(\omega)$  varies continuously between that for the ICS and HCS in Fig. 4 (a) and (b).

*Conclusions* We emphasize that particulate systems over most of the  $\Delta\phi$  and  $T_0$  plane near jamming display nonharmonic vibrational response, *i.e.* the density of vibrational frequencies  $D(\omega^v)$  from the Fourier transform of the velocity autocorrelation function is continuous, not a set of discrete, sharp peaks at the dynamical matrix eigenfrequencies  $\omega_k^d$  and differs from other measures of the vibrational response. This implies that when particulate systems are excited by a single mode  $\omega_k^d$ , the response rapidly spreads to a continuous spectrum of other modes. This result has important consequences for acoustic transmission [15] and thermal transport [16] in jammed solids. However, there is a wide swath of parameter space (corresponding to HCS) where the frequencies associated with displacement correlation matrix do not depend on  $\Delta\phi$  or  $T_0$ .  $D(\omega^s)$  in this regime differs from  $D(\omega^d)$  for  $\Delta\phi > 0$  at  $T_0 = 0$  and from  $D(\omega^s)$  for hard-particle liquids. These results underscore the importance of measuring directly the vibrational response for MS packings instead of inferring it from linear response.

We acknowledge support from NSF Grant No. CBET-0968013 (MS), DTRA Grant No. 1-10-1-0021 (CO and TB), and Yale University (CS). This work also benefited from the facilities and staff of the Yale University Faculty of Arts and Sciences High Performance Computing Center and the NSF (Grant No. CNS-0821132) that in part funded acquisition of the computational facilities.

[1] E. W. Montroll, *J. Chem. Phys.* **10** (1942) 218.

[2] K. N. Pathak, *Phys. Rev.* **139** (1965) A1569.

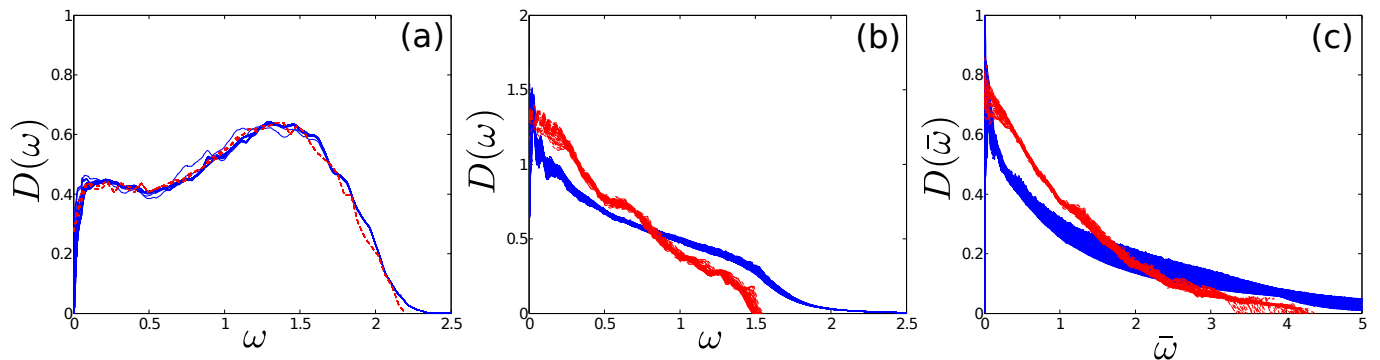


FIG. 4: (Color online) Binned density of vibrational frequencies  $D(\omega^v)$  (blue solid lines) and  $D(\omega^s)$  (red dashed lines) for more than 75 sets of parameters in the (a) ICS and (b) HCS regimes, as well as (c) hard-particle liquids for  $N = 128$ . For HPL,  $\omega$  is normalized by the average frequency  $\bar{\omega} = \omega / \langle \omega \rangle$ .

- [3] C. Brito, O. Dauchot, G. Biroli, and J.-P. Bouchaud, *Soft Matter* **6** (2010) 3013.
- [4] K. Chen, W. G. Ellenbroek, Z. Zhang, D. T. N. Chen, P. J. Yunker, S. Henkes, C. Brito, O. Dauchot, W. van Saarloos, A. J. Liu, and A. G. Yodh, *Phys. Rev. Lett.* **105** (2010) 025501.
- [5] C. F. Schreck, T. Bertrand, C. S. O'Hern, and M. D. Shattuck, *Phys. Rev. Lett.* **107** (2011) 078301.
- [6] A. J. Liu and S. R. Nagel, *Ann. Rev. Condens. Matt. Phys.* **1** (2010) 347.
- [7] M. van Hecke, *J. Phys.: Condens. Matt.* **22** (2010) 033101.
- [8] C. Brito and M. Wyart, *J. Chem. Phys.* **131** (2009) 024504.
- [9] G.-J. Gao, J. Blawdziewicz, and C. S. O'Hern, *Phys. Rev. E* **74** (2006) 061304.
- [10] A. Tanguy, J. P. Wittmer, F. Leonforte, and J.-L. Barrat, *Phys. Rev. B* **66** (2002) 174205.
- [11] G.-J. Gao, J. Blawdziewicz, C. S. O'Hern, and M. D. Shattuck, *Phys. Rev. E* **80** (2009) 061304.
- [12] A. Ikeda, L. Berthier, and G. Biroli, *J. Chem. Phys.* **138** (2013) 12A507.
- [13] S. Henkes, C. Brito, and O. Dauchot, *Soft Matter* **8** (2012) 6092.
- [14] M. Schmiedeberg, T. K. Haxton, S. R. Nagel, and A. J. Liu, *Europhys. Lett.* **96** (2011) 36010.
- [15] C.-J. Hsu, D. L. Johnson, R. A. Ingale, J. J. Valenza, N. Gland, and H. A. Makse, *Phys. Rev. Lett.* **102** (2009) 058001.
- [16] V. Vitelli, N. Xu, M. Wyart, A. J. Liu, and S. R. Nagel, *Phys. Rev. E* **81** (2010) 021301.